

A Fluorescent Microtiter Plate-Based Detection Platform for Hydrogen Peroxide, Glucose, and Lactate

John J. Galligan, Antje J. Baeumner, and Axel Duerkop*

Hydrogen peroxide (H₂O₂) is an important small metabolite often quantified with commercially available multistep fluorescence-based assays. A new microtiter plate (MTP)-based platform that allows a rapid, one-step assay with a ratiometric readout function is developed. Specifically, 10-Acetyl-3,7-dihydroxyphenoxazine (ADHP) in a polyurethane-based hydrogel sensor membrane is embedded. For a ratiometric set-up, the membranes are loaded with polystyrene nanoparticles containing a Cy5-based reference which allowed for the compensation for variations in membrane thickness. These knife-coated μm-thin films are mounted onto bottomless MTPs with double-sided adhesive tape. Optimized membranes provide measurement times of 3 min upon sample

addition and a limit of detection (LOD) in phosphate-buffered saline that is 10x lower than that of the ADHP-using Amplex Red commercial kit of 100 nmol L⁻¹ H₂O₂. These ADHP hydrogels can be stored at room temperature for at least 22 months. Horseradish peroxidase (HRP) is nanospotted alone or together with either lactate oxidase or glucose oxidase for the detection of H₂O₂, lactate, and glucose, respectively. With 50 v% glycerol as cryoprotectant in the spotting solution, the HRP ADHP platform is stable for at least 13 weeks at -20 °C. Enhanced simplicity and comparable performance to multistep assays suggest that the platform can simplify MTP-based assays in the future.

1. Introduction

Hydrogen peroxide (H₂O₂) is a compound found in a variety of applications as reagent, disinfectant, or metabolite in numerous enzyme-catalyzed reactions. In the first cases, the analysis is important to determine concentrations beyond the desired or permitted limit values and thus to avert any harmful effects.^[1] In case of the latter, H₂O₂ is a particularly interesting analyte as a marker for a variety of diseases^[2] and due to the availability of a range of H₂O₂-generating enzymes that provide access to concentrations of multiple precursor analytes.^[3]

Electrochemical^[4] and optical^[5] methods are the two most commonly developed approaches to detect H₂O₂. Depending on the setup, electrochemical approaches either monitor the oxidation or reduction of H₂O₂. To overcome the high potentials needed, a plethora of approaches both for novel materials and surface modifications for electrodes and new electrocatalysts for the electrochemical detection of H₂O₂ have been developed making electrochemical detection a viable option for rapid and on-site tests.^[4,6,7]

In a nonautomated setting, optical H₂O₂-quantification is often achieved with commercially available colorimetric or fluorescent assays in microtiter plates (MTPs) with desirably low limit of detections (LODs).^[8] In case of colorimetry, 3,3',5,5'-Tetramethylbenzidine^[9] or 2,2'-azino-bis(3-ethylbenzothiazoline-6-sulfonic acid)^[10] are typically applied, for fluorescent approaches, although also usable for colorimetric^[11] and electrochemical detection,^[12] the predominant dye is 10-Acetyl-3,7-dihydroxyphenoxazine (ADHP) better known by its commercial name Amplex Red.^[13] In presence of H₂O₂ and a suitable catalyst or enzyme, here horseradish peroxidase (HRP), a 1:1 stoichiometric, irreversible reaction takes place from colorless and nonfluorescent ADHP to pink-colored resorufin (**Figure 1**), which shows a fluorescence emission peak at 585 nm with a 572 nm excitation maximum.^[14]

ADHP is ideally stored at -20 °C, light-protected,^[15] and separately from horseradish peroxidase (HRP) which is preferably stored at 4 °C, due to the slow oxidation to resorufin occurring in presence of HRP, even without any H₂O₂ present which makes the development of one-step biosensors and assays difficult.^[11] Hence, the combination of the ADHP-HRP couple results in additional thawing, dilution, and mixing steps for any assay that takes more time and in turn reduces the amount of sample throughput and considerably increases the chance for human error. However, considering the instability of dilute H₂O₂,^[16] the quantification of low concentrations is time-critical to avoid an underestimation of H₂O₂.

In the past, hydrogel membranes have been shown to be the ideal environment for the storage of (bio)-recognition probes.^[17] Hydrogels have also been used for a variety of applications in the development of detection methods, such as containing the catalytically active component,^[18] as H₂O₂

J. J. Galligan, A. J. Baeumner, A. Duerkop
 Institute of Analytical Chemistry
 Chemo- and Biosensors
 University of Regensburg
 Universitätsstraße 31, 93053 Regensburg, Bavaria, Germany
 E-mail: axel.duerkop@chemie.uni-regensburg.de

 Supporting information for this article is available on the WWW under <https://doi.org/10.1002/anse.202500060>

 © 2025 The Author(s). Analysis & Sensing published by Wiley-VCH GmbH. This is an open access article under the terms of the Creative Commons Attribution License, which permits use, distribution and reproduction in any medium, provided the original work is properly cited.

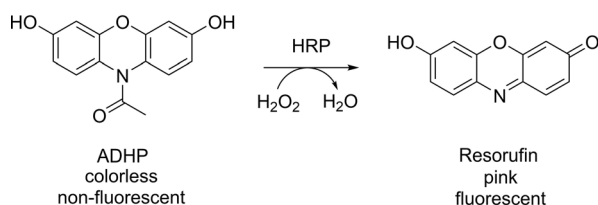


Figure 1. HRP-catalyzed reaction of colorless, nonfluorescent ADHP to pink, fluorescent resorufin in presence of H_2O_2 .

scavenger^[19] or for housing the probe.^[20] Hydrogels and polymers that do not require chemical or physical crosslinking can usually be easily applied onto surfaces by knife coating, also known as doctor blade coating^[21] to form versatile sensor membranes of μm -thickness.

We therefore investigated an approach toward an all-in-one ratiometric fluorescent H_2O_2 MTP detection platform that is simple to produce and is based on the fast and efficient release of ADHP from a thin film of commercially available polyurethane hydrogel after a single sample-addition step. By nanospotting HRP together with H_2O_2 generating enzymes, we achieve sufficient separation of enzyme and dye to combine assay times of few minutes with LODs for H_2O_2 down to $10 \text{ nmol}\cdot\text{L}^{-1}$. To extend the stability of the spotted enzyme for storage, we used 50 v% glycerol as cryoprotectant to investigate the stability for a duration of 13 weeks.

2. Experimental Section

Detailed protocols on membrane production, the used devices, and all the measurements performed can be found in the SI. Bidistilled water was used for any aqueous solutions, if not stated otherwise. All organic solvents used were of analytical grade or better quality and used without further purification. Produced dye stocks membranes and spotted plates were stored light-protected.

2.1. Chemicals

HydroMed D640 was supplied from AdvanSource biomaterials, Mitsubishi Chemical America Inc. (Wilmington, USA); H_2O_2 -solution (34.5–36.5 %), glycerol ($\geq 99\%$), Polystyrene (average $M_w \approx 280000 \text{ g}\cdot\text{mol}^{-1}$), horseradish peroxidase, and glucose oxidase were obtained from Sigma–Aldrich, Merck KGaA (Darmstadt, Germany); lactate oxidase was purchased from Sorachim SA (Lausanne, Switzerland); and 10-Acetyl-3,7-dihydroxyphenoxazine (ADHP, 99.5%) was purchased from Synchem UG & Co KG (Felsberg–Altenburg, Germany). S0982, 4,5:4',5'-Dibenzo-1,1'-dibutyl-3,3,3',3'-tetramethylindadicarbocyanine hexafluorophosphate was supplied by FEW-chemicals GmbH (Bitterfeld–Wolfen, Germany). Sodium dodecyl sulfate (SDS, $\geq 99.0\%$) was obtained from AppliChem GmbH (Darmstadt, Germany)

Phosphate-buffered saline (PBS, pH 7.4) was prepared from NaCl (p.A.), KCl (p.A.) from Carl Roth GmbH + Co. KG (Karlsruhe, Germany), Na_2HPO_4 (p.A.), and KH_2PO_4 (p.A.) from

Merck KGaA (Darmstadt, Germany). The pH was adjusted to 7.4 with NaOH-solution ($1 \text{ mol}\cdot\text{L}^{-1}$, Titripur) also from Merck KGaA.

2.2. Special Labware

Nonsterile black bottomless 96-well MTPs were purchased from Greiner Bio-One GmbH (www.gbo.com). 3 M Double-sided adhesive tape with polyester backing GPT-020F, transparent, $100 \text{ mm} \times 50 \text{ m}$, 0.202 mm was obtained from SKS GmbH (www.shop-sks.com). Biaxially oriented PET-membrane roll with a thickness of $125 \mu\text{m}$ was purchased from Goodfellow GmbH (www.goodfellow.com). Spectra/Por 4 dialysis membrane tubing MWCO:12-14 kD was obtained from Carl Roth GmbH & Co KG (www.carlroth.com). Life science sealing films for storage and automation, aluminum, self-adhesive were bought from Brand GmbH & Co KG (www.brand.de).

2.3. Dye-Loaded Polystyrene Nanoparticle (PSNP) Synthesis

Dye-loaded PSNPs were synthesized following a modified protocol published by Bartoš et al.^[22] which is a polymerization free version of the surfactant-enabled microemulsion method.^[23,24] In short, aqueous sodium lauryl sulfate (SDS)-solution (14.0 mL , $1.00 \text{ mg}\cdot\text{mL}^{-1}$, 48.5 mmol), PS in toluene (average $M_w \approx 280000$, $1800 \mu\text{L}$, $96.6 \text{ mg}\cdot\text{mL}^{-1}$, 174 mg), and S0982 in toluene ($100.0 \mu\text{L}$, $17.29 \text{ mg}\cdot\text{mL}^{-1}$, 1.729 mg) were filled in a glass vial with snap cap. Under vigorous stirring, the solution was sonicated with a sonication tip at 60 W with 60 one-second pulses a total of three times. In between each sonication procedure, the emulsion was stirred with a sealed lid for 1 h. Afterwards, the solvent was allowed to evaporate at RT with an open lid under stirring for 48 h. The residual aqueous phase was then dialyzed over 72 h with bidistilled water (800 mL). The dialysate was exchanged five times. Particle suspensions were stored light-protected in ambient conditions. Particles were analyzed with fluorescence spectroscopy, dynamic light scattering, and transmission electron microscopy (TEM).

2.4. Membrane Production

For a typical membrane, ADHP-stock in DMSO ($20 \mu\text{L}$, $50 \text{ mmol}\cdot\text{L}^{-1}$, $1 \mu\text{mol}$) was added to D640 (6 g 10% , in EtOH/ H_2O 9:1 v/v). The solution was vigorously stirred light-protected for 10 min. Precleaned dust-free $15 \times 34 \text{ cm}$ PET-substrate was fixed to a vacuum bed, and the D640-ADHP cocktail (spacer was set to a thickness of $30 \mu\text{m}$) was knife-coated on top. The film was then dried for 2 h at 37°C , laser-cut (compare SI Figure 2, Supporting Information), and fixed to the bottom of a self-made sticky MTP (compare Figure 2 + SI Figure 1, Supporting Information).

2.5. Spotting Procedure

Nanospotting was done with a scienion nanospotter (www.scienion.com) equipped with a coated NDC-M nozzle. Following a standard startup and priming procedure, the required spotting

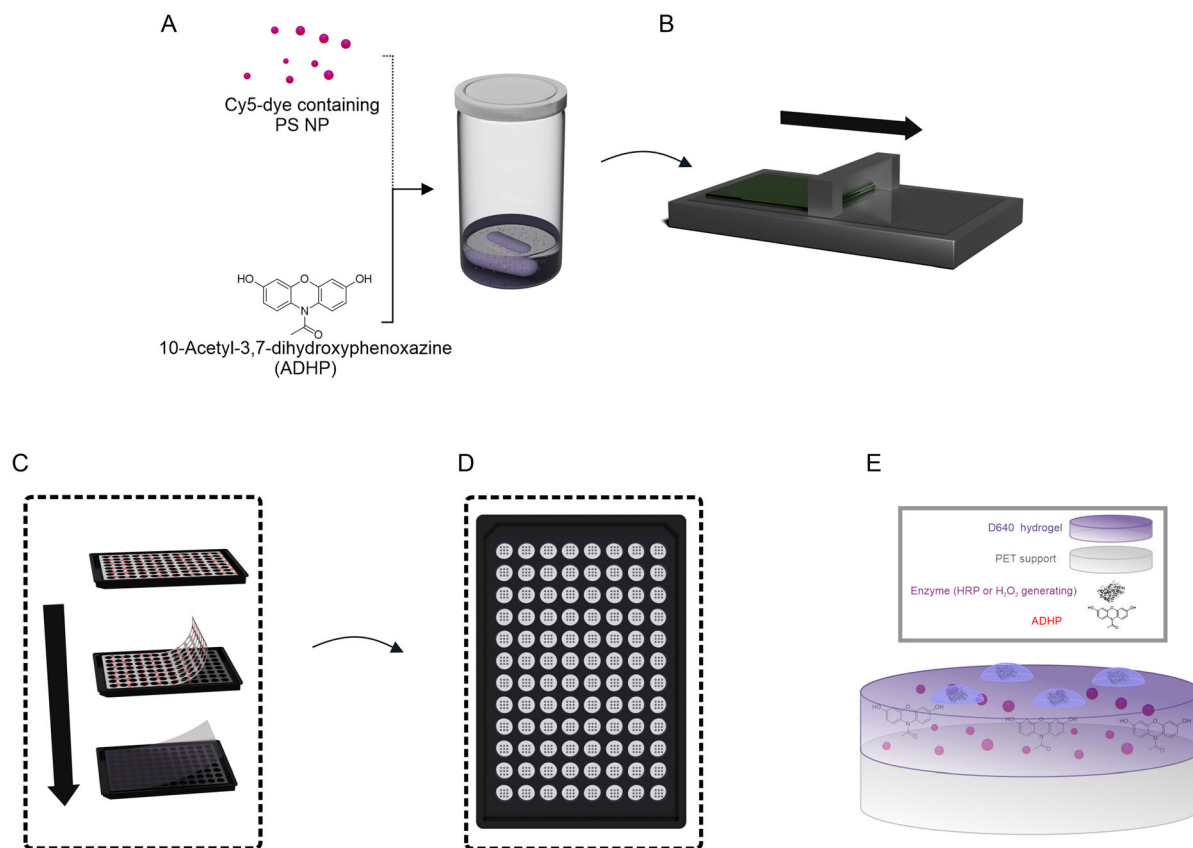


Figure 2. A) Luminescent HP probe and reference dye particles are dissolved in hydrogel B) from which membranes are knife-coated and dried on PET. C) Sensing membranes are laser cut and stuck onto the bottom of in-house made sticky bottom MTPs. D) Enzyme is spotted on top of the sensing membrane in the wells. E) Schematic cross-section of stacked sensor membrane with support, hydrogel, dye NPs, and the probe ADHP.

volume (25–50 nL) is set by adjusting pressure and valve-opening time (i.e., 8% pressure $\hat{=}$ 37 kPa, 350 μ s pulse time results in \approx 30 nL spots, SI Figure 18, Supporting Information). The solution to be nanospotted is aspirated (in PBS pH 7.4: HRP 22.5 U·mL⁻¹, GOx 0.2 U·mL⁻¹, LOx 0.4 U·mL⁻¹), the tip subsequently dipped into water to remove enzyme-solution contaminating the outside of the tip, and 20 jets are ejected to remove any water aspirated by capillary forces. The corresponding number of spots is then dispensed into each selected well on the MTP-mounted membrane following the production, as described in section 2.4. For further functionalization, additional enzyme (GOx, LOx) was spotted in a second step following the same procedure as for HRP.

3. Results and Discussion

3.1. MTP Design and Knife Coating

The necessity of several predilution and preparation steps before measurement with commercial ADHP tests makes the usage of the latter time and cost-intensive, and in case of automation, requires more sophisticated procedures and extra steps. In designing the new platform technology, the goal was to reduce this to ideally one step, in which the sample is prediluted in buffer for pH adjustment and then just added to an MTP containing all

the other required reagents and catalysts. Key to the new platform is the use of a hydrogel membrane in which the assay reagents can be embedded and simultaneously separated from each other. Thus, a fluorescent detection probe and PSNPs with an integrated reference dye were added into a hydrogel matrix, and enzymes were simply nanospotted on the dried film. Thus, all three components are stored with sufficient separation, and the system can easily be mass-produced providing increased stability of all components in the dried state and in the correct concentration for the desired assay. Upon addition of sample or buffer, the enzymes are dissolved, the fluorescent probe is released, and the reference dye remains protected from exposure to the analyte.

While there are a variety of methods to apply hydrogels and polymers for the development of sensors,^[21] we decided to use knife-coating, also known as doctor blade coating, as it enables both fast prototyping and parameter screening on small-scale coaters but is also accessible to large-scale industrial roll-to-roll production. For this approach, we also developed and prepared sticky MTPs from bottomless MTPs with double-sided adhesive tape stuck to the bottom of the well walls by laser-cutting double-sided adhesive tape to fit the wall of the wells (compare SI chapter I.V.I). The knife-coated membranes can then be laser-cut and mounted on the bottom of these in-house modified bottomless 96-well MTPs, allowing a fast, simple, and streamlined production of a detection platform for a widespread system.

The transparent coating substrate and hydrogel allow for the detection with both top optics, and, if available, bottom optics measurement in an MTP-reader.

Looking for a suitable polymer or hydrogel as matrix, we tested several polymer/solvent combinations. We primarily focused on commercially available polymers that do not require chemical or photocatalytic crosslinking or curing, but only solvent evaporation after coating. For this study, we investigated polyvinyl acetate/cellulose acetate (PVAc/CA), LRP t 7016, D4, and D640.

PVAc/CA has been used in literature as coating for enzymatic sensors,^[25] we investigated both DMF/H₂O and cyclohexanone (Chon) as solvent candidates. PVAc/CA 10w% DMF/H₂O 9:1 v/v (SI Figure 4G, and 6G, Supporting Information) shows very little fluorescence intensity increase over time with no clear dependence of H₂O₂ concentration, which suggests very little and insufficient release of ADHP. The kinetic curve of the PVAc/CA 10w% Chon/H₂O 99:1 v/v-membranes indicates a better reagent release of ADHP (SI Figure 4F and 6F, Supporting Information), however, no specificity toward the concentration of H₂O₂ makes this polymer combination unsuitable.

LRP t 7016, which is an amorphous poly(L-lactide-co-D, L-lactide-co-PEG) triblock-polymer dissolved in THF/H₂O 99:1 has the disadvantage of no release of ADHP (SI Figure 4H and 6H, Supporting Information).

D4 and D640 are both polyurethane-based hydrogels, whereby D4 in particular is often used as matrix for the development of optical sensors.^[26–29] In comparison to D4, D640 exhibits a larger pore size, due to its increased maximum water content. Both can be dissolved in a variety of solvents. However, using aqueous-ethanolic mixtures as solvents is particularly interesting as toxic, cancerogenic, and high-boiling solvents can be avoided. In this context, alcohols in the 9:1 mix were tested with D4 as solvent component to determine the effect of the type of alcohol on the response. We investigated the effect of different alcohols (ethanol, isopropanol, and tert-butanol) and dimethyl formamide (DMF) as polar aprotic solvent in the coating mix toward the release of the dye. In general, D4 shows a good reagent release and response time/kinetic curve. There was, however, no major

difference in the response time for the different solvents, with the last concentration reaching the equilibrium after about 10 min (SI Figure 4 A–D and 6 A–D, Supporting Information). Isopropanol as co-solvent seems to reduce the background signal (SI Figure 4 C and 6C, Supporting Information) but has no other positive effect apart from that. However, as it is known to form light-induced peroxides under ambient conditions,^[30] it would not be the optimal choice in this platform set-up.

D640 shows both a very fast response time of only around 3 min (SI Figure 4E and 6E, Supporting Information) and linear response range up to 5 $\mu\text{mol}\cdot\text{L}^{-1}$ H₂O₂ with a calculated LOD of 0.09 $\mu\text{mol}\cdot\text{L}^{-1}$ ($3\cdot\sigma_{\text{blank}}\cdot\text{slope}^{-1}$ compare Figure 3) and a linear range up to 5 $\mu\text{mol}\cdot\text{L}^{-1}$ already surpassing the given LOD of the Thermo Fisher commercial kit of 0.1 $\mu\text{mol}\cdot\text{L}^{-1}$ (reported as 10 pmol per 100 μL in the manual). As a result, we chose D640 as thin-film matrix for the storage and application of ADHP over D4 here because of the fast and effective reagent release.

An issue commonly observed and known for ADHP in the classical liquid assay that also impacts the membrane set-up, is a fluorescence intensity decrease with higher H₂O₂ concentrations as a nonfluorescent product is formed.^[13] This formation can result in an incorrect determination and thus underestimation of high H₂O₂ concentrations. To broaden the dynamic range in that higher concentration, thicker membranes were studied as these could host overall more dye. However, too thick membranes show a slower release of the dye (SI Figure 7, Supporting Information). Also, the amount of dye in the membrane was optimized, as with too high concentrations the gel becomes overloaded with dye and DMSO affecting the drying process and thus performance. In the end, the best overall results were achieved with 20 μL of ADHP-stock (containing 50 $\text{mmol}\cdot\text{L}^{-1}$ ADHP) per 6 g of hydrogel-solvent mix. Below this concentration, the analytical range is reduced, above the hydrogel becomes overloaded and cannot release the dye as efficiently and fast after drying.

Deviations in membrane thickness led to deviations in H₂O₂ detection as the ADHP concentration varies accordingly. This is especially apparent in manual lab-based knife coating processes and likely less so in a commercial roll-to-roll manufacturing

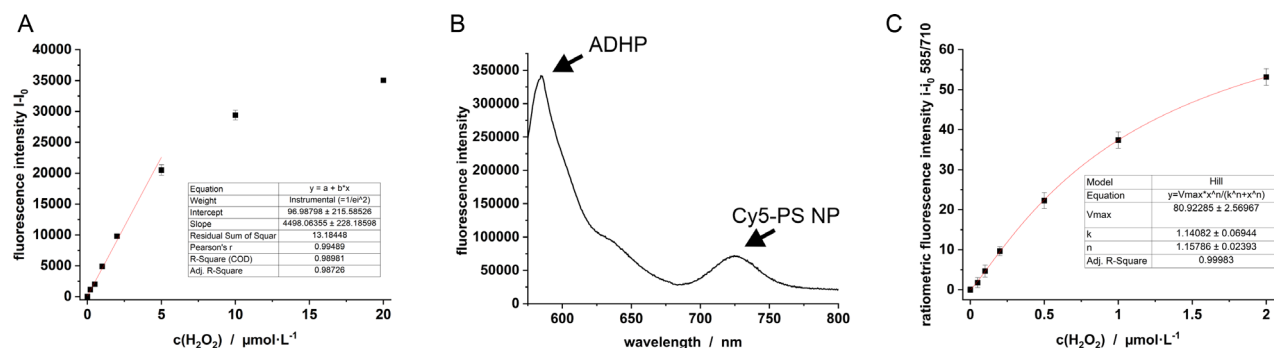


Figure 3. A) Dose-response curve of ADHP in D640 toward increasing concentrations of H₂O₂ with linear fit. Biotek plate reader $\lambda_{\text{exc.}} = 560$ nm, 10 nm slit, $\lambda_{\text{em.}} = 585$ nm, 10 nm slit, N = 3, T = 37 °C. B) Cuvette-based emission spectrum of ADHP with H₂O₂, HRP, and S0982-loaded PSNPs in PBS pH 7.4 showing the emission maxima of ADHP at 585 nm and the dye-loaded PSNPs at 725 nm. Edinburgh F55 $\lambda_{\text{exc.}} = 560$ nm, 1 nm slit, $\lambda_{\text{em.}} = 570$ –800, 1 nm slit, 0.1 s dwell time, 0.5 nm steps, 5 repeats. C) Dose-response curve of the ratiometric signal of ADHP in sensor membrane composed of D640 with dye-loaded PSNPs, 10 mU HRP per well, and increasing concentrations of H₂O₂. Biotek plate reader $\lambda_{\text{exc.}} = 560$ nm, 10 nm slit, $\lambda_{\text{em.}} = 585$ nm and 710 nm, each with 10 nm slit, N = 3, T = 37 °C.

process. Nonetheless, ratiometric detection approaches can avoid any problems caused by changes in membrane height of dye distribution. A group of cyanine dyes was identified as a good match for ADHP. They can still be excited with the 560 nm excitation wavelength useful for resorufin but show emission at around 700 nm which is far enough away from the 585 nm resorufin emission. To avoid their oxidation by H_2O_2 and HRP, a hydrophobic cyanine without sulfo-moieties, 4,5,4', 5'-Dibenzo-1,1'-dibutyl-3,3,3', 3'-tetramethylindadicarbocyanine was used. Since it could not be dissolved in the dye membrane cocktail it was loaded into PSNPs (SI Figure 12 and 19, Supporting Information) which protected it from oxidation. When stored light-protected at room temperature the dye in the particles was stable for at least 15 months. This enabled ratiometric detection of H_2O_2 , both in a purely liquid assay in cuvettes (Figure 3B) and membrane-based in the MTP (Figure 3C). The increased reliability afforded by this ratiometric approach also enabled an LOD of $0.05 \mu\text{mol}\cdot\text{L}^{-1}$ surpassing the previous LOD even further ($3\cdot\sigma_{\text{blank}}\cdot\text{slope}^{-1}$).

3.2. Development of Nanospotted Enzyme-Based Assays

For a one-step assay, it was investigated how enzymes could be integrated with the membrane platform. Integration of the

enzyme in a membrane layer works well, but it requires very high amounts of $80 \text{ U}\cdot\text{g}^{-1}$ or more enzyme in the coating solution (SI Figure 8, Supporting Information) which indicates the enzyme not being released from the membrane as efficiently as the dye. The amount of enzyme could be dramatically reduced via nanospotting. A 3x3 matrix fitting 9 spots can easily be achieved per well (Figure 4A). The small volume of $\approx 30 \text{ nL}$ per spot or $\approx 270 \text{ nL}$ per well reduces hydrogel swelling and thus interaction of the enzyme and the dye. This approach can easily be adapted to co-spot more than one enzyme or modify the hydrogel surface with other molecules. The amount of HRP spotted was optimized to avoid increased background due to unspecific oxidation of ADHP or slowed response. Optimal conditions included 4 HRP spots ($\approx 30 \text{ nL}$, $22.5 \text{ U}\cdot\text{mL}^{-1}$, SI Figure 10, Supporting Information) leaving place for 5 extra spots containing other enzymes like GOx or LOx. With the 4 spots of HRP a very good spectral intensity distinction between the background fluorescence caused by the unspecific oxidation of ADHP by HRP and with $0.1 \mu\text{mol}\cdot\text{L}^{-1} \text{H}_2\text{O}_2$ added is clearly possible (Figure 4B). With a full dose-response curve accessible after only 3 min assay time (Figure 4C), in the smaller concentration range below $0.1 \mu\text{mol}\cdot\text{L}^{-1}$ (Figure 4D) a distinction between the blank and $0.02 \mu\text{mol}\cdot\text{L}^{-1}$ is clearly possible.

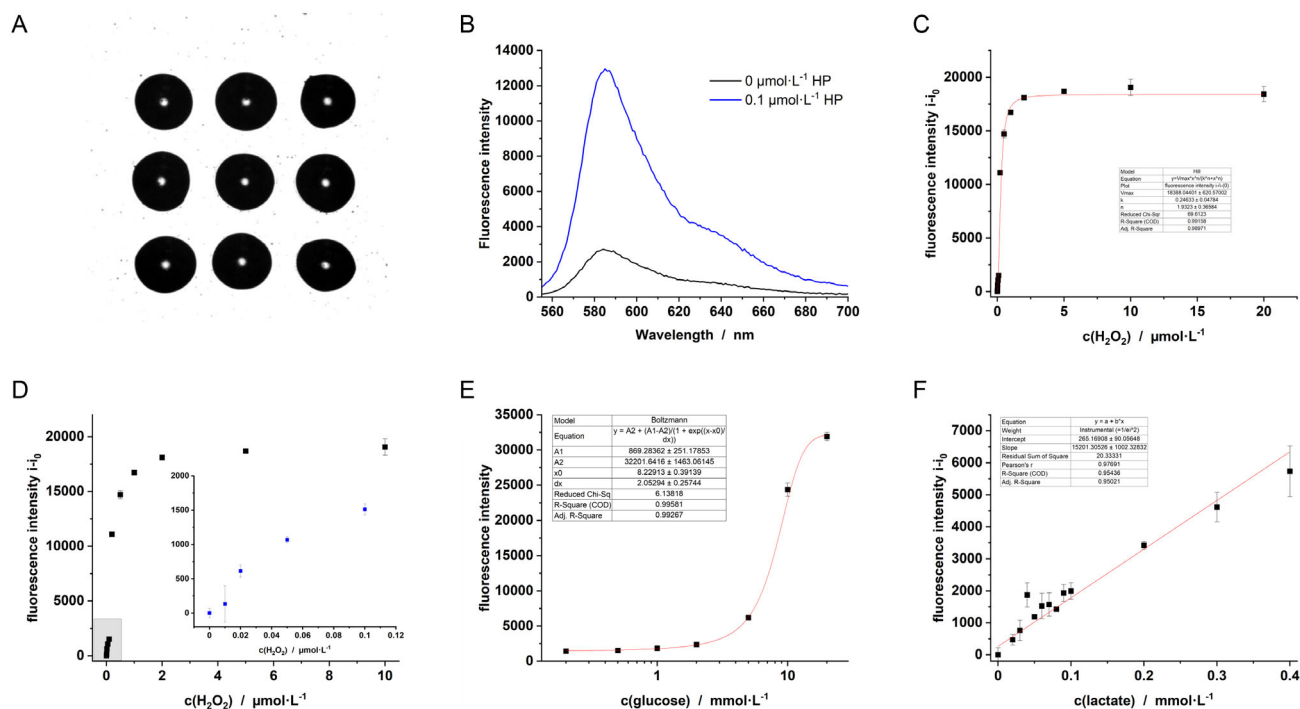


Figure 4. A) Top head image of 9 50 nL HRP spots in a MTP well. B) Fluorescence spectra of ADHP in D640 ($\lambda_{\text{exc.}} = 550\text{--}10 \text{ nm}$) and HRP (4 spots, 30 nL per spot, $22.5 \text{ U}\cdot\text{mL}^{-1}$) spotted with $0 \mu\text{mol}\cdot\text{L}^{-1}$ (black) and $0.1 \mu\text{mol}\cdot\text{L}^{-1} \text{H}_2\text{O}_2$ in PBS pH 7.4. C) Dose-response curve with Hill fit of ADHP in D640 ($\lambda_{\text{exc.}} = 560\text{--}10 \text{ nm}$, $T = 37 \text{ }^\circ\text{C}$, $\lambda_{\text{em.}} = 585\text{--}10 \text{ nm}$, $N = 4$) and HRP (4 spots, 30 nL per spot, $22.5 \text{ U}\cdot\text{mL}^{-1}$) spotted with increasing concentrations of H_2O_2 in PBS pH 7.4 after 3 min assay time. D) Enlarged section (blue squares $0 - 0.1 \mu\text{mol}\cdot\text{L}^{-1}$) dose-response curve section of ADHP in D640 ($\lambda_{\text{ex}} = 560\text{--}10 \text{ nm}$, $\lambda_{\text{em}} = 585\text{--}10 \text{ nm}$, $N = 4$), and HRP (4 spots, 30 nL per spot, $22.5 \text{ U}\cdot\text{mL}^{-1}$) spotted with increasing concentrations of H_2O_2 in PBS pH 7.4, LOD = $0.01 \mu\text{mol}\cdot\text{L}^{-1}$. E) Dose-response curve of ADHP in D640 ($\lambda_{\text{exc.}} = 560\text{--}10 \text{ nm}$, $T = 37 \text{ }^\circ\text{C}$, $\lambda_{\text{em.}} = 585\text{--}10 \text{ nm}$, $N = 4$) and HRP (4 spots, 30 nL per spot, $22.5 \text{ U}\cdot\text{mL}^{-1}$)/GOx (4 spots, 30 nL per spot, $0.2 \text{ U}\cdot\text{mL}^{-1}$) spotted with increasing concentrations of glucose in PBS pH 7.4, LOD = $4 \text{ mmol}\cdot\text{L}^{-1}$. F) Dose-response curve of ADHP in D640 ($\lambda_{\text{exc.}} = 560\text{--}10 \text{ nm}$, $T = 37 \text{ }^\circ\text{C}$, $\lambda_{\text{em.}} = 585\text{--}10 \text{ nm}$, $N = 4$) and HRP (4 spots, 30 nL per spot, $22.5 \text{ U}\cdot\text{mL}^{-1}$)/LOx (4 spots, 30 nL per spot, $0.4 \text{ U}\cdot\text{mL}^{-1}$) spotted with increasing concentrations of lactate in PBS pH 7.4, LOD = $0.04 \text{ mmol}\cdot\text{L}^{-1}$. (C–F) Biotek plate reader $\lambda_{\text{exc.}} = 560 \text{ nm}$, 10 nm slit, $\lambda_{\text{em.}} = 585 \text{ nm}$, 10 nm slit, $N = 4$, $T = 37 \text{ }^\circ\text{C}$.

The linear regression in this area even results in a calculated LOD of $0.01 \mu\text{mol}\cdot\text{L}^{-1} \text{H}_2\text{O}_2$.

Second, the enzymes GOx or LOx were co-spotted into the wells for the detection of glucose and lactate, respectively. The concentration of the enzymes and the number of spots per well were optimized with respect to detecting within the physiological range. Here, the best results were achieved with 4 spots ($\approx 30 \text{ nL}$) of GOx with $0.2 \text{ U}\cdot\text{mL}^{-1}$ (SI Figure 11A, Supporting Information) and $0.4 \text{ U}\cdot\text{mL}^{-1}$ LOx (SI Figure 11B, Supporting Information). The entire system was then applied for glucose and lactate detection in buffer. Glucose could be detected in the range from $4\text{--}20 \text{ mmol}\cdot\text{L}^{-1}$ (Figure 4E), lactate in the range of $0.04\text{--}0.4 \text{ mmol}\cdot\text{L}^{-1}$ (Figure 4F). Considering the reported successful use of ADHP together with HRP and H_2O_2 producing enzymes in a variety of challenging biological matrices,^[31–34] application of the platform in such systems should be possible. When using H_2O_2 -spiked milk diluted 1:10 in PBS in the wells as a complex and highly scattering matrix, an LOD of $0.13 \mu\text{mol}\cdot\text{L}^{-1}$ and a linear range of up to at least $2 \mu\text{mol}\cdot\text{L}^{-1}$ were possible after 3 min assay time (SI Figure 21, Supporting Information).

3.3. Stability

Initial experiments of ADHP-membranes with spotted HRP in PBS showed complete oxidation of ADHP at 4°C and declines of the activity over a course of 4 weeks at RT and -20°C (SI Figure 14, Supporting Information). In the case of the latter two, the addition of fresh enzyme allowed for the assay to proceed, which indicates the degradation of the enzyme. It is assumed that at RT, both the increased temperature and the lacking humidity cause denaturation. At -20°C , the denaturation is either caused by the formation of ice crystals or the slow evaporation of H_2O from structurally important coordination positions within the active center of the enzyme.^[35] At 4°C , the enzyme can still catalyze the unspecific oxidation of ADHP, albeit slowly. Furthermore, it is assumed that the humidity present allowed some hydrogel swelling and interaction of dye and enzyme leading to the formation of resorufin over time. To improve on storage stability of the enzyme known additives (50 v% glycerol, 10 w% dextran, and $500 \text{ mmol}\cdot\text{L}^{-1}$ sucrose) were added to the spotting solution, ensuring that good dispensibility or the spotting solution was maintained. The composition of 50 v% glycerol in the spotting solution decreases the freezing point to about -40°C ^[36] preventing damage caused by the formation of ice crystals.^[37] Dextran has been used as alternative to glycerol in literature to prevent hemolysis of red blood cells during freezing,^[38] and sucrose is a common cryoprotectant used for the cryopreservation by vitrification.^[39] Surprisingly, dextran, sucrose, and PBS fail in long-term stability protection as about 50% of signal response is lost within the first week of storage at -20°C and are in fact hardly discernable from the unspecific oxidation of ADHP by HRP without H_2O_2 (SI Figure 16, Supporting Information). In contrast, HRP spotted with 50 v% glycerol showed a good stability over a course of 13 weeks with a coefficient of variance of 9%. Considering the random distribution of data, the variance is likely caused by

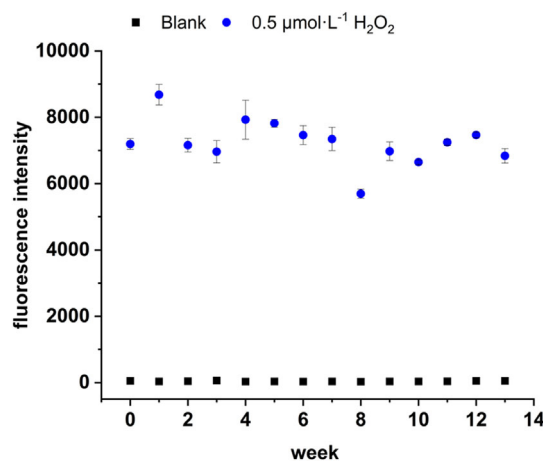


Figure 5. Stability of ADHP membranes with spotted HRP (3 spots, 30 nL per spot, $22.5 \text{ U}\cdot\text{mL}^{-1}$) in 50 v% glycerol stored at -20°C ($\lambda_{\text{exc.}} = 560\text{--}10 \text{ nm}$, $T = 37^\circ\text{C}$, $\lambda_{\text{em.}} = 585\text{--}10 \text{ nm}$, $N = 3$).

membrane thickness variation in production or the variation in spotted HRP-stock and not by significant reduction in enzyme activity (Figure 5). The facts that standalone membranes containing ADHP could still be used after 22 months with fresh HRP (SI Figure 15, Supporting Information) and no significant reduction of signal intensity of HRP with glycerol as cryoprotectant suggest the possibility of extended long-term storage, which will be studied further in the future.

3.4. Material Cost of Production

Currently commercially available ADHP assay kits retail in Europe at around 500 € or USD for 500 tests or about 1 € or USD per test. Material required for the production of the developed MTP-based platform only costs 7.29 € per MTP (96 tests) or about 0.08 € per test, despite the small-scale purchase of production materials (SI Table 1, Supporting Information), suggesting significantly lower material prices in case of large-scale production.

4. Conclusion

An MTP-based hydrogel sensor membrane platform was developed containing ADHP, reference particles, and nanospotted enzymes for the ratiometric fluorometric detection of H_2O_2 . When coupled with H_2O_2 -generating enzymes, detection of glucose in physiologically relevant range and lactate in a 1:10 dilution thereof was demonstrated. The presented platform drastically reduces assay preparation steps, with only sample addition after predilution in buffer which could be shown for milk as complex and highly scattering matrix and is very attractive for automation setups. Depending on the membrane quality, thickness, dye, and enzyme load, very fast H_2O_2 assays of 3 min are possible with LODs one order of magnitude lower than published for the commercial assay in solution. At low material costs of 0.08 € per test, this platform technology can provide a drastically simplified

analysis strategy for high-throughput screening of all assays in which H₂O₂ is produced.

Key design criteria were the separation of ADHP and HRP to avoid nonspecific reactions, the pore sizes of the membrane to enable a rapid release of the dye, the implementation of a reference dye to increase reliability, and nanospotting of the enzymes involved to obtain fast response times and low material consumption. Considering the release mechanism of the hydrogel membrane, the platform might also be suitable to host a variety of other responsive dyes and probes.

Acknowledgements

The authors would like to thank Christoph Bühler for the TEM-images of the PSNPs and Prof. Dr. Reiner Müller for giving us access to the rheology measurement equipment.

Open Access funding enabled and organized by Projekt DEAL.

Conflict of Interest

The authors declare no conflicts of interest.

Data Availability Statement

The data that support the findings of this study are available from the corresponding author upon reasonable request.

Keywords: Amplex Red · H₂O₂ · hydrogels · hydrogen peroxide · sensors

- [1] A. S. Ivanova, A. D. Merkuleva, S. V. Andreev, K. A. Sakharov, *Food Chem.* **2019**, *283*, 431.
- [2] F. Rezende, R. P. Brandes, K. Schröder, *Antioxid. Redox Signaling* **2018**, *6*, 585.
- [3] J. J. Galligan, A. J. Baeumner, A. Duerkop, *TrAC, Trends Anal. Chem.* **2024**, *180*, 117948.
- [4] W. Chen, S. Cai, Q.-Q. Ren, W. Wen, Y.-D. Zhao, *Analyst* **2012**, *137*, 49.
- [5] M. Moßhammer, M. Kühn, K. Koren, *Chemosensors* **2017**, *5*, 28.
- [6] J. E. Giaretta, H. Duan, F. Oveissi, S. Farajikhah, F. Dehghani, S. Naficy, *ACS Appl. Mater. Interfaces* **2022**, *14*, 20491.
- [7] K. Dhara, D. R. Mahapatra, *J. Mater. Sci.* **2019**, *54*, 12319.
- [8] M.-J. Lee, J.-A. Song, J.-H. Choi, J.-H. Shin, J.-W. Myeong, K.-P. Lee, T. Kim, K.-E. Park, B.-K. Oh, *Biosensors* **2023**, *13*, 289.
- [9] P. E. Thomas, D. Ryan, Wayne Levin, *Anal. Biochem.* **1976**, *75*, 168.
- [10] R. E. Childs, W. G. Bardsley, *Biochem. J.* **1975**, *145*, 93.
- [11] I. Sanz-Vicente, I. Rivero, L. Marcuello, M. P. Montano, S. de Marcos, J. Galbán, *Anal. Bioanal. Chem.* **2023**, *415*, 1777.
- [12] N. Gajovic-Eichelmann, F. F. Bier, *Electroanalysis* **2005**, *17*, 1043.
- [13] M. Zhou, Z. Diwu, N. Panchuk-Voloshina, R. P. Haugland, *Anal. Biochem.* **1997**, *253*, 162.
- [14] D. Dębski, R. Smulik, J. Zielonka, B. Michałowski, M. Jakubowska, K. Dębowska, J. Adamus, A. Marcinek, B. Kalyanaraman, A. Sikora, *Free Radical Biol. Med.* **2016**, *95*, 323.
- [15] B. Zhao, F. A. Summers, R. P. Mason, *Free Radical Biol. Med.* **2012**, *53*, 1080.
- [16] M. Ventura, in *41st AIAA/ASME/SAE/ASEE Joint Propulsion Conference & Exhibit. 41st AIAA/ASME/SAE/ASEE Joint Propulsion Conference & Exhibit, Tucson, Arizona, American Institute of Aeronautics and Astronautics, Reston, Virginia* **2005**.
- [17] D. Zhai, B. Liu, Y. Shi, L. Pan, Y. Wang, W. Li, R. Zhang, G. Yu, *ACS Nano* **2013**, *7*, 3540.
- [18] D. Calabria, A. Pace, E. Lazzarini, I. Trozzi, M. Zangheri, M. Guardigli, S. Pieraccini, S. Masiero, M. Mirasoli, *Biosensors* **2023**, *13*, 650.
- [19] J. Huang, Y. Zheng, H. Niu, J. Huang, X. Zhang, J. Chen, B. Ma, C. Wu, Y. Cao, Y. Zhu, *Adv. Healthcare Mater.* **2023**, *13*, e2302328.
- [20] A. Dutta, U. Maitra, *ACS Sens.* **2022**, *7*, 513.
- [21] M. Bauer, A. Duerkop, A. J. Baeumner, *Anal. Bioanal. Chem.* **2023**, *415*, 83.
- [22] D. Bartoš, L. Wang, A. S. Anker, M. Rewers, O. Aalling-Frederiksen, K. M.Ø. Jensen, T. J. Sørensen, *PeerJ Mater. Sci.* **2022**, *4*, e22.
- [23] K. Landfester, *Angew. Chem. Int. Ed.* **2009**, *48*, 4488.
- [24] K. Landfester, *Annu. Rev. Mater. Res.* **2006**, *36*, 231.
- [25] T. Tsuchida, K. Yoda, *Clin. Chem.* **1983**, *29*, 51.
- [26] L. Ding, S. Chen, W. Zhang, Y. Zhang, X. Wang, *Anal. Chem.* **2018**, *90*, 7544.
- [27] A. Ø. Tjell, B. Jud, R. Schaller-Ammann, T. Mayr, *Sens. Actuators, B.* **2023**, *400*, 134904.
- [28] S. Bidmanova, M.-S. Steiner, M. Stepan, K. Vymazalova, M. A. Gruber, A. Duerkop, J. Damborsky, Z. Prokop, O. S. Wolfbeis, *Anal. Chem.* **2016**, *88*, 6044.
- [29] M. Moßhammer, M. Strobl, M. Kühn, I. Klimant, S. M. Borisov, K. Koren, *ACS Sens.* **2016**, *1*, 681.
- [30] C. E. Redemann, *J. Am. Chem. Soc.* **1942**, *64*, 3049.
- [31] R. Gaikwad, P. R. Thangaraj, A. K. Sen, *Sci. Rep.* **2021**, *11*, 2960.
- [32] M. F. Santillo, Y. Liu, *J. Pharmacol. Toxicol. Methods* **2015**, *76*, 15.
- [33] Z. Zou, C. B.-D. Pury, A. K. Hewavitharana, S. S. Al-Shehri, J. A. Duley, D. M. Cowley, P. Koorts, P. N. Shaw, N. Bansal, *Food Chem.* **2021**, *336*, 127689.
- [34] A. H. Palamakumbura, P. C. Trackman, *Anal. Biochem.* **2002**, *300*, 245.
- [35] B. Darbyshire, *Cryobiology* **1975**, *12*, 276.
- [36] L. B. Lane, *Ind. Eng. Chem.* **1925**, *17*, 924.
- [37] H. H. Gorris, D. R. Walt, *J. Am. Chem. Soc.* **2009**, *131*, 6277.
- [38] C. Pellerin-Mendes, L. Million, M. Marchand-Arvier, P. Labrude, C. Vigneron, *Cryobiology* **1997**, *35*, 173.
- [39] G. D. Elliott, S. Wang, B. J. Fuller, *Cryobiology* **2017**, *76*, 74.

Manuscript received: April 24, 2025

Revised manuscript received: June 6, 2025

Version of record online: